Cells Lacking Pfh1, a Fission Yeast Homolog of Mammalian Frataxin, Display Constitutive Activation of the Iron Starvation Response

Natalia Gabrielli, José Ayté and Elena Hidalgo[1]

[1]From the Oxidative Stress and Cell Cycle Group, Departament de Ciències Experimentals i de la Salut[1], Universitat Pompeu Fabra, C/ Dr. Aiguader 88, 08003 Barcelona, Spain

Running title: *Proteome of frataxin homolog in fission yeast*

To whom correspondence should be addressed: Elena Hidalgo, Address correspondence to: Elena Hidalgo, Universitat Pompeu Fabra, C/ Dr. Aiguader 88, 08003 Barcelona, Spain, Tel.: 34-93-316-0848; Fax.: 34-93-316-0901; E-mail: elena.hidalgo@upf.edu

Keywords: Friedreich ataxia, frataxin, iron homeostasis, oxidative stress, Fep1, Php4, Grx4, *S. pombe*

Background: Defects in the protein frataxin give rise to Friedreich ataxia.
Results: A new Friedreich ataxia model using fission yeast has been generated, and its phenotype and proteome characterized.
Conclusion: Frataxin absence triggers a complete iron starvation program, sufficient to generate all the associated respiratory defects.
Significance: Our new model system may contribute to decipher the role of frataxin.

SUMMARY

Friedreich ataxia is a genetic disease caused by deficiencies in frataxin. This protein has homologues not only in higher eukaryotes, but also in bacteria, fungi and plants. The function of this protein is still controversial. We have identified a frataxin homolog in fission yeast, and have analyzed whether its depletion leads to any of the phenotypes observed in other organisms. Cells deleted in *pfh1* are sensitive to growth under aerobic conditions, display increased levels of total iron, hallmarks of oxidative stress such as protein carbonylation, decreased aconitase activity and lower levels of oxygen consumption compared to wild-type cells. This mitochondrial protein seems to be important for iron and/or reactive oxygen species homeostasis. We have analyzed the proteome of cells devoid of Pfh1, and determined that gene products up- and down-regulated upon iron depletion in wild-type cells are constitutively misregulated in this mutant. Due to the particular signalling pathway components governing the iron starvation response in fission yeast, our experiments suggest that cells lacking Pfh1 display a decrease of cytosolic available iron which triggers activation of Grx4, the common regulator of the iron starvation gene expression program. Our *Schizosaccharomyces pombe* Δ*pfh1* strain constitutes a new and useful model system to study Friedreich ataxia.

Friedreich ataxia is an inherited autosomal recessive disease causing degeneration in the central and peripheral nervous system, cardiomyopathy, skeletal abnormalities and increased risk of diabetes mellitus (1-4). A decreased expression of a highly conserved nuclear-encoded mitochondrial protein, known as frataxin, causes Friedreich ataxia. In 98% of the cases, an unstable hyper-expansion of a GAA triplet repeat in the first intron of the gene is the most common genetic mutation (2,5). The expanded GAA repeat impairs frataxin transcription by adopting an abnormal triple helical structure.

This disease is thought to be the consequence of a mitochondrial defect related to iron metabolism. Thus, the cardiac tissues from patients with Friedreich ataxia contain iron deposits, are deficient in respiratory complexes I, II and III and aconitase activities and have reduced mitochondrial DNA (6,7).

The finding of iron accumulation in the hearts of both patients and mouse models (6,8,9), suggests that excess free iron is involved in the production of reactive oxygen species and is responsible for the oxidative damage to iron sulfur clusters (ISCs) and loss of mitochondrial DNA (10).

Iron is a vital metal for most biological organisms and participates in an astonishing array of biological reactions such us DNA synthesis, cell cycle progression and respiration (11). Nevertheless, this redox-active transition metal presents a dilemma to cells, because iron can also catalyze the deleterious oxidation of biomolecules via Haber-Weiss/Fenton chemistry when combined with reactive oxygen species (ROS) (12). Accordingly, concentration of iron in cells is tightly regulated by control of its uptake and intracellular storage (13).

Frataxin is a mitochondrial iron binding protein and its primary function remains controversial, since iron homeostasis, intracellular fluctuations of ROS, oxidation and damage of ISCs and mitochondrial dysfunctions are all intimately linked, and it is not trivial to establish the sequential order of events leading to the disease. Homologues to human frataxin have been found in bacteria, fungi and plants (for a review, see 14). In particular, unicellular model systems are being exploited to determine the origin of the pleiotropic phenotypes displayed by patients. In particular, *Saccharomyces cerevisiae* cells deficient in the frataxin homologue Yfh1 are unable to carry out oxidative phosphorylation, lose mitochondrial DNA (15), display impaired iron efflux out of mitochondria with a consequent accumulation of iron in this compartment (16), suffer iron depletion in the cytosol, show elevated expression of high affinity iron uptake, exhibit heme deficiency (17) and have an increased sensitivity to oxidative stress. Additional properties of these *ΔYFH1* mutant cells include defects in the synthesis of ISCs with a consequent deficiency of ISC-containing proteins and loss of respiratory competence. Furthermore, *in vitro* studies indicate that Yfh1 can bind iron and deliver it to Isu1 (ISC assembly scaffold protein) (18,19). The phenotypes caused by decreased levels of frataxin point to the notion that it plays a role in ISC synthesis and mitochondrial and cellular iron misregulation with a consequent oxidative stress. However, studies on mice and yeast also show that the loss of ISCs precedes iron accumulation (9,20), so that the anomalies may not be a direct result of iron-induced oxidative damage. Furthermore, studies using an *S. cerevisiae* model of conditional expression of frataxin demonstrated that the primary consequence of frataxin depletion is to trigger up-regulation of the iron transport system before affecting iron sulfur enzyme activities (21).

The success of previous simple models of Friedreich ataxia prompted us to investigate whether we could isolate a *Schizosaccharomyces pombe* strain mimicking the phenotypes observed in other organisms. We have found an open-reading frame (ORF), *pfh1,* coding for the fission yeast homologue of human frataxin. We have constructed a strain carrying a deletion of the gene, and found phenotypes resembling those of other Friedreich ataxia model systems. Despite the great amount of data obtained with previous model systems, the analysis of the proteome of our frataxin-deficient strain has provided us with new data and has prompted us to discard previous hypothesis, such as the possible role of frataxin on ISC biogenesis.

EXPERIMENTAL PROCEDURES

Alignment of frataxin sequence - The alignment of frataxin protein sequence of *S. pombe, S. cerevisiae* and human isoform 1 was performed by multiple sequence alignment with hierarchical clustering software (22).

Growth conditions and yeast strains - Cells were grown in rich medium (YE5S) or synthetic minimal medium (MM) as described previously (23). Yeast cells were grown in anaerobic liquid cultures in bottles filled to the top (50 ml) with YE5S until exponential phase, to the OD_{600} indicated for each method. We used wild-type strains 972 (h^-) and 975 (h^+) (24), and AV18 (*h⁻ sty1::kanMX6*) (25). To construct *S. pombe* strains with specific loci deleted, we transformed wild-type strain 972 with linear fragments containing ORFs fused to *kanMX6* or *natMX6*, obtained by PCR amplification using ORF-specific primers and plasmids pFA6a-kanMX6 (26) or pFA6a-natMX6 (27) as templates, and we obtained strains NG60 (h^-

pfh1::natMX6) and NG40 (*h⁻ php4::kanMX6*) by transforming as previously described in (28); NG60 was isolated under anaerobic growth conditions (Forma Anaerobic, System Thermo electron corporation). *S. pombe* strain NG1 (*h⁻ fep1::kanMX6*) was selected from an isolate of a deletion collection (29) (http://pombe.bioneer.co.kr/introduction/ResearchPurpose.jsp) after eliminating auxotrophies by crossing it with 972 strain. To obtain NG147 (*h⁻ pfh1::natMX6 fep1::kanMX6*) and NG148 (*h⁻ pfh1::natMX6 php4::bleoMX*), we crossed NG60 with the triple mutant NG141 (*h⁺ fep1::kanMX6 php4::bleoMX grx4::natMX6*), and they were isolated by tetrad dissection and selected under anaerobic conditions. To construct NG142 (*h⁻ pfh1::GFPkanMX6),* an *S. pombe* strain expressing green fluorescent protein (GFP) tagged to Pfh1, we transformed the wild-type strain 975 *(h⁺)* (24) *with* linear fragments containing *pfh1::GFP::kanMX6* obtained by PCR amplification using *pfh1*-specific primers and plasmids pFA6a-GFP(S65T)-kanMX6 as template (26). Origins and genotypes of strains used in this study are outlined in supplemental Table S1.

Solid sensitivity assay - In order to analyze sensitivity to different agents on plates, *S. pombe* strains were grown and spotted as described (30). Serial diluted cells were spotted into MM or YE5S plates containing or not the indicated concentrations of hydrogen peroxide (H_2O_2), deferroxamine mesylate (Dx) (Sigma) or iron ($FeCl_3.6H_2O$, Sigma). The spots were allowed to dry, and the plates were incubated at 30°C during 2 to 3 days under aerobic or anaerobic conditions.

Labeling of total disulfides for 1D electrophoresis analysis - Protein extracts of exponentially growing *S. pombe* cells were obtained and labeled as previously described (31).

Colorimetric assay for iron quantification - Yeast cells were grown in YE5S anaerobic liquid cultures (50 ml). Cells were washed twice with PBS buffer pH 7.4 and treated as described (32) using ferrozine (Fluka). Absorbance of iron-chelator complex was recorded at OD_{565} in a UV-visible Ultraspec 2100-pro (Amersham Biosciences) spectrophotometer. The accuracy of the assay was improved by subtracting non-specific absorbance recorded at OD_{680}. The number of cells was calculated from OD_{600} (OD_{600} 0.5 = $1x10^7$ cells/ml). Standard curves were prepared from 10-40 nmoles of $FeCl_3$ dissolved in 3% nitric acid. All chemicals (except ferrozine from Fluka) were purchased from Sigma and resuspended in ultrapure water obtained from a Millipore Milli-Q Advantage. Data was obtained from three independent experiments and are expressed as mean ± SEM.

Protein carbonylation - The detection method was performed as described (33).

Enzymatic activity assay for aconitase - In order to perform aconitase enzymatic activity assay for wild type and Δ*pfh1* strains*, S. pombe* cells were grown in YE5S in anaerobic conditions to an OD_{600} of 0.5. Aconitase activity was assayed as described (34) following method 2. Aconitase activity can be measured spectrophotometrically at 340 nm using citrate as the substrate of aconitase, and the isocitrate formed is then converted to α-ketoglutarate by $NADP^+$-dependent isocitrate dehygrogenase. Yeast cells were washed once with PBS buffer pH 7.4. Total protein extracts were prepared by homogenization with glass beads in Tris buffer (50 mM Tris-HCl pH 7.6, 1 mM cysteine, 1 mM citrate, 0.5 mM $MnCl_2$). Insoluble material was removed by centrifugation during 10 min at 16,000 g at 4ºC. Supernatants were collected and 10 µl of the total extract were mixed with 90 µl of reaction buffer [50 mM Tris-HCl, pH 7.4, 30 mM sodium citrate, 0.5 mM $MnCl_2$, 0.2 mM $NADP^+$, isocitrate dehygrogenase (2 units/ml, Fluka)]. Absorbance at 340 nm (ε_{340}=6.22 mM^{-1} cm^{-1}) was recorded by UV-visible Spectrophotometer (UV-1700 Pharma Spec Shimadzu). Data was obtained from three independent experiments and are expressed as mean ± SEM.

Measurement of oxygen consumption - Oxygen consumption of approximately 10^7 cells in 1 ml, collected from anaerobic cultures at an OD_{600} of 0.5, was measured as described before (35).

Fluorescence microscopy - Cells expressing Pfh1-GFP were grown in YE5S till an OD_{600} of 0.5. They were then incubated with

0.1 µg/ml of MitoTracker Red CMXRos (Invitrogen) during 30 min. Cells were pelleted and resuspended in YE5S. Fluorescence microscopy and image capture was performed as previously described (36).

RNA analysis - Total RNA from exponentially growing *S. pombe* cells in YE5S was extracted, processed and transferred to a membrane as previously reported (37). Membranes were hybridized with [α-^{32}P] dCTP-labeled *pfh1, pap1, trr1, trx1, tpx1, ctt1, zwf1, caf5, obr1, SPCC663.08c, fio1, str3, pcl1* and *isa1* probes. Ribosomal RNAs and *act1* were used as loading controls.

Cell extracts and immunoblot analysis of Pap1 - Preparation of *S. pombe* trichloroacetic acid (TCA) protein extracts to measure Pap1 concentration was performed as described before (38). Samples were separated by 8% SDS-PAGE. Gels were transferred to membranes, and they were probed with a polyclonal anti-Pap1 anti-serum and anti-Sty1 anti-serum (as loading control) (36)

Growth Curves - Yeast cells were grown in YE5S and the cultures of NG60, NG147 and NG148 strains were grown anaerobically. The initial OD_{600} of the growth curves was 0.1 and recording of the growth curves was performed as described (30).

Quantification of proteins by dimethyl labeling - 50 ml of wild type and *Δpfh1* cells were grown to exponential phase (OD_{600} 1.0) anaerobically. Cells were passed to aerobic conditions with shaking for 3 h, which did not significantly affect viability of the cultures (supplemental Fig. S1). Cells were collected after addition to the cultures of 100% TCA to a final concentration of 10%, pellets were washed with 20% TCA and cells were lysed by vortexing with glass beads in 250 µl of 12.5% TCA. Cell lysates were then pelleted, washed twice in cold acetone and dried. Each pellet was resuspended in 500 µl of 200 mM Tris-HCl pH 8.5, 6 M urea, 5 mM EDTA and 0.05% SDS. Protein concentration was determined by Bradford assay. 25 µg of protein of each sample were reduced by addition of 15 µl of 10 mM DTT in 200 mM triethyl-ammonium bicarbonate (TEAB) (1 hour at 37ºC) and then alkylated by adding 15 µl of 20 mM iodoacetamide in 200 mM TEAB (30 min at room temperature). Upon reduction and alkylation, protein extracts were diluted in 200 mM TEAB to a final urea concentration of 1 M. At this point protein extracts were trypsinized (Promega), and tryptic peptides were labeled with either normal (wild type) or deuterium labeled (*Δpfh1*) formaldehyde (Sigma Aldrich), respectively (39,40). A modification was added to the dimethyl labeling protocol (40): the reaction mixture was not acidified prior to mixing, but instead 8 µl of 1% ammonia solution was added, as described (31). All the details regarding mass spectrometers used and data processing has been published elsewhere (31)

Analysis of dimethyl labeled proteins - For the analysis of dimethyl labeled proteins Proteome Discoverer v1.2.0.208 (Thermo Fisher Scientific, Bremen, Germany) was used to extract MS/MS spectra which were queried using Mascot v2.3, as described (31). Protein ratios are reported as the median of the measured peptide ratios for a given protein. Regarding data analysis, database searches MS/MS spectra were extracted as previously reported (31). For protein accession and gene identification (supplemental Tables S2 to S5), peptides were searched against *S. pombe* GeneDB (http://old.genedb.org/genedb/pombe/, Wellcome Trust Sanger Institute).

RESULTS

Identification and deletion of the gene pfh1, which codes for the fission yeast frataxin homolog - We searched the *S. pombe* genome for genes with homology to the human frataxin gene, and found an ORF (*SPCC1183.03c*) coding for a 158-aa long polypeptide sharing 42% and 44% of protein identity with human and *S. cerevisiae* frataxin, respectively (Fig. 1A). We named the protein Pfh1 (*pombe* frataxin homologue 1), following the nomenclature used for the *S. cerevisiae* frataxin (yeast frataxin homologue, Yfh1). *YFH1* diverged from the human gene earlier in evolution than *S. pombe pfh1* (Fig. 1A), which further motivated us to analyze the effect of *pfh1* deletion on the cell's physiology. We generated a strain lacking the whole ORF by genetic recombination, as shown by Northern blot analysis (Fig. 1B), and had to perform the

selection of the deleted clones under semi-anaerobic conditions. The substitution of the whole *yfh1* ORF by an antibiotic resistance cassette was checked by PCR (data not shown). When anaerobic cultures of strain Δ*pfh1* were spotted on agar plates, we observed severe growth defects in the presence of oxygen (Fig. 1C). In fact, even the viability of liquid cultures of strain Δ*pfh1* was severely compromised when grown under aerobic conditions, as shown in Fig. 1D. We also determined that cells lacking Pfh1 display sensitivity to exogenous oxidative stress (Fig. 1E). These results are consistent with an essential role of Pfh1 in cellular fitness, since it is required for respiratory growth and for survival in front of intrinsic (Fig. 1CD) or extrinsic (Fig. 1E) accumulation of ROS.

Phenotypic characterization of strain Δpfh1 - Since our Δ*pfh1* strain seemed to share the sensitivity to aerobic growth of other Friedreich ataxia model systems, we tested whether it also recapitulated some of the characteristic features related to iron homeostasis and mitochondrial metabolism. We detected over 3-fold increases in total iron in extracts from strain Δ*pfh1* compared to wild-type cells (Fig. 2A). The strain, either before or after a transient shift to aerobic conditions, displayed hallmarks of oxidative stress, such as increased levels of reversibly oxidized thiols (Fig. 2B) or protein carbonylation (Fig. 2C). The activity of the ISC-containing protein aconitase was also significantly reduced in the mutant (Fig. 2D), and respiratory competence was also severely affected as determined by measuring oxygen consumption (Fig. 2E). All these features have also been reported for previous models of Friedreich ataxia, and confirmed the relevance of our newly developed system. Consistently, protein Pfh1 displayed mitochondrial localization, as previously reported for human and *S. cerevisiae* frataxin proteins (Fig. 2F).

Characterization of the proteome of Δpfh1 cells - To decipher the role of Pfh1 in the cell physiology, we analyzed the protein composition of total cell extracts of cells lacking Pfh1 and of wild-type cells, when anaerobic cultures were shifted for 3 hours to aerobic conditions (supplemental Fig. S1). Tryptic peptides derived from cell extracts were labeled with either normal (wild type) or deuterium labeled (*Δpfh1*) formaldehyde. Peptides were then mixed and analyzed by LC-MS/MS, as described in Experimental Procedures. The complete list of proteins misregulated in *Δpfh1* cells is provided in supplemental Tables S2 and S3. A total of 58 proteins were over-expressed more than 1.5-fold, and 71 were down-regulated more 2-fold, in extracts from *Δpfh1* cells when compared to wild-type extracts (Table 1). The expression of more than half of these misregulated proteins (39 with lower expression and 35 with higher expression; Table 1) have not been identified as regulated by a common transcription factor, as far as we know. However, the expression of 52 proteins (32 with lower expression and 20 with higher expression; Table 1) is regulated upon iron starvation, at least at the gene level (41). Furthermore, 9 of the proteins over-expressed in *Δpfh1* cells are regulated by the transcription factor Pap1 (Table 1), at least at their mRNA levels (42).

Cells lacking Pfh1 display increased expression of some Pap1-dependent proteins - At least 9 proteins whose expression depends on the transcription factor Pap1 are over-represented in extracts from cells lacking Pfh1 (supplemental Table S4). In response to H_2O_2, the transcription factor Pap1 up-regulates transcription of genes required for adaptation to oxidative stress and for tolerance to toxic drugs. H_2O_2 induces oxidation of Pap1, its nuclear accumulation, and expression of more than fifty Pap1-dependent genes, some of which are antioxidant genes and others drug resistance genes (Fig. 3A) (36,42). We have recently reported that the ability of Pap1 to bind and activate the second subset of promoters, those of drug tolerance genes, is independent on Pap1 oxidation. Thus, nuclear localization of non-oxidized Pap1 or over-expression of the protein is sufficient to trigger activation of drug resistance genes, but Pap1 has to be not only nuclear but also oxidized to bind to another transcription factor, Prr1, and activate antioxidant genes (43).

We first checked by Northern blot analysis whether the expression of the genes coding for some of the Pap1-dependent proteins

over-expressed in *Δpfh1* extracts are also up-regulated under basal conditions. As shown in Fig. 3B, the levels of Pap1-dependent drug resistance mRNAs are up-regulated by aerobic growth even prior to the addition of H_2O_2 in cells lacking Pfh1, but not the antioxidant ones such as *trr1*. Since the presence of Pap1 at the nucleus can also be accomplished by over-expression of the transcription factor, with the subsequent activation of drug tolerance genes (43), we tested whether the mRNA for *pap1* (Fig. 3C) and/or the levels of Pap1 protein (Fig. 3D) were elevated in strain *Δpfh1*. Surprisingly, both *pap1* mRNA (Fig. 3C) and Pap1 protein levels (Fig. 3D) are 3-10-fold higher in this strain background than in wild-type cells, which could explain the constitutive activation of some drug resistance genes (Fig. 3E). Further work will be required to understand how up-regulation of *pap1* levels is occurring upon deletion of *pfh1*; this is the first reported genetic mutation that affects Pap1 activity at the level of transcription. Oxidation of the transcription factor is not altered in this mutant (data not shown), which discards enhanced H_2O_2 levels triggering its activation.

Cells lacking Pfh1 display increased expression of proteins normally up-regulated upon iron starvation - As shown in supplemental Table S4, the genes of 20 proteins over-expressed in strain *Δpfh1* are normally triggered in wild-type cells upon iron starvation, at least at their mRNA levels (41). In *S. pombe*, addition of chelators such as dipyridyl (DIP) to cell cultures induces pronounced changes in the gene expression program, which are dependent on Grx4, Fep1 and Php4 (Fig. 4A). Briefly, the inactivation of Fep1 and activation of Php4 transcriptional repressors mediate the cellular response to iron deficiency, by either up- or down-regulating, respectively, the expression of genes (44). Thus, upon low iron conditions Fep1 is released from promoters of genes involved in iron uptake, such as *fio1* or *str3* (Fig. 4AB) (45). As shown in Fig. 4B, the expression of the Fep1 repressor-dependent *fio1* and *str3* genes is de-repressed under basal conditions in cells lacking Pfh1, similarly to what occurs in cells devoid of the Fep1 repressor. Consistently, a double delete *Δpfh1 Δfep1* strain has the same phenotype as cells lacking only Pfh1. It is important to point out that *Δfep1* cells are not sensitive to grow under aerobic conditions, as shown on solid plates (Fig. 4C) or in liquid cultures (Fig. 4D), which indicates that the constitutive activation of iron uptake genes observed in *Δpfh1* cells does not contribute to their sensitivity to grow under aerobic conditions.

Cells lacking Pfh1 display decreased levels of proteins normally down-regulated upon iron starvation - As shown in supplemental Table S5, 32 proteins down-represented in extracts from strain *Δpfh1* are also down-regulated at their gene levels upon iron starvation, most of them in a Php4-dependent manner. Thus, upon low iron, Php4 accumulates at the nucleus and represses transcription of genes coding for iron-storage or iron-consuming proteins (Fig. 4A) (46). First of all, we confirmed by Northern blot that not only protein levels but also mRNA levels for some Php4-dependent genes, such as *pcl1* and *isa1*, are constitutively low in *Δpfh1* cells (Fig. 5A). It is important to point out that many of the genes down-regulated by Php4 upon iron starvation are ISC- or iron-containing proteins, and many of them are essential (supplemental Table S5). Since deletion of the *php4* gene, coding for a repressor, leads to the lack of iron-starvation-dependent gene repression (Fig. 5A) (41), we tested whether the oxygen-sensitive phenotype of cells lacking Pfh1 could be alleviated by further deletion of the *php4* gene. As shown in Fig. 5A, expression of *pcl1* and *isa1* was constitutively up-regulated in the double knock-out strain, as expected. Furthermore, the sensitivity to grow under aerobic conditions was partially suppressed in the double mutant as shown both on solid plates (Fig. 5B) and in liquid cultures (Fig. 5C). Excess iron or addition or iron chelators did not significantly improve or impaired the growth of *Δpfh1* cells (Fig. 5B). Therefore, the constitutive down-regulation observed in strain *Δpfh1* of some Php4 genes, many of which are essential, is partially, but not totally, contributing to the severe phenotype of our Friedreich ataxia model. It is also worth mentioning that genes coding for the ISC-containing proteins aconitase are also Php4-

dependent and are therefore down-regulated in our *Δpfh1* strain; this fact would be sufficient to justify the low activity levels of this and other ISC-containing proteins in this genetic background (Fig. 2D).

The transcriptome of Δpfh1 cells resembles that of Δgrx4 Δfep1 cells - As explained above, both the transcriptome (as observed by Northern blots) and the proteome of cells lacking Pfh1 are very similar to that of wild-type cells under iron limitation. Thus, iron import is exacerbated and iron storage and iron-containing proteins are down-regulated. Since the glutaredoxin Grx4 is the common link between up- (Fep1-dependent) and down-(Php4-dependent)-regulation of transcription under iron deprivation (Fig. 4A), our frataxin homolog could be participating in signaling by regulating Grx4. However, deletion of the gene coding for this glutaredoxin does not lead to the same transcriptome changes as deletion of *pfh1* (Fig. 6A). Indeed, the only strain that misregulates the iron regulon in the same directions as strain *Δpfh1* is the double delete *Δgrx4 Δfep1* (Fig. 6A). We interpret these results by hypothesizing that the absence of Pfh1 does not directly participate in the signaling cascade leading to the complete iron-starvation gene program; instead, it may really trigger an iron starvation situation, which should consequently activate Grx4. It is worth mentioning that *Δgrx4 Δfep1* cells also display severe growth phenotypes in the presence of oxygen (Fig. 6B). That indicates that many of the phenotypes of our Friedreich ataxia model system, strain *Δpfh1,* are caused by the misregulation of the iron regulon itself, and in particular by the constitutive Php4-dependent repression of many essential ISC-containing proteins.

DISCUSSION

Deficiencies in frataxin give origin to Friedreich ataxia. We have here developed a new model system to study the molecular events leading to the disease: fission yeast cells lacking Pfh1 display all hallmarks of other previously reported model systems. Importantly enough, the function of frataxin (and therefore the molecular events leading to the disease in the absence of this protein) is still controversial, and our new model system may shed light into the essential function of this protein under aerobic conditions.

S. cerevisiae Yfh1, the budding yeast frataxin homolog, was early reported to directly participate in ISC biogenesis, since aconitase activity was reduced in cells lacking the protein, and this inactivation seemed to precede iron accumulation (9,47). In particular, yeast frataxin has been suggested to participate in ISC maturation as an iron donor, based on its reported interaction with Isu1 (19,48). However, it has also been demonstrated that restricting oxidative damage, either by decreasing ROS production (49) or by diminishing available iron (50), prevents aconitase inactivation. Furthermore, a conditional knock-down of Yfh1 expression has allowed establishing the order of sequential events occurring upon frataxin depletion, indicating that induction of iron import is a primary event leading to the late inactivation of ISC-containing proteins (21). Our results suggest that the low levels of aconitase activity in cells lacking Pfh1 are a consequence of the earlier activation of Php4 repressor, which in wild-type cells lowers expression of most ISC-containing proteins in an iron starvation-dependent manner. Therefore, our work does not support the idea that frataxin is required for ISC biogenesis, but rather directly or indirectly participates in iron-sensing and signaling.

As explained above, the fission yeast gene expression program upon iron starvation is governed by Grx4, which ultimately is responsible of both up- and down-regulation of several genes. Downstream of Grx4, the inactivation of Fep1 and activation of Php4 transcriptional repressors mediate the cellular response to iron deficiency (44). Briefly, when iron is experimentally depleted by the use of chelators Fep1 is released from promoters of genes involved in iron uptake (45), while Php4 accumulates at the nucleus and represses transcription of genes coding for iron-storage or iron-consuming proteins (46). Importantly enough, Grx4 is the real sensor of iron deprivation, probably through its ISC (our unpublished results). However, the apo-protein does not mimic an iron starvation response, indicating that the loss of the ISC is not the

mechanism by which wild-type Grx4 becomes active (our unpublished results). Similarly, cells devoid of Grx4 only mimic the iron starvation response with regard to gene-down-regulation by Php4, but cannot trigger activation of Fep1-dependent genes (Fig. 6A). As we have shown here, cells devoid of Pfh1 display all hallmarks of an iron deprivation situation, which can hardly be accomplished by genetic modulation of iron sensing/signaling components. In fact, only cells carrying double deletion of *grx4* and *fep1* display a similar transcriptome and phenotype as Δ*pfh1* cells (Fig. 6AB). Pfh1 could modulate Grx4 activity by, for instance, stabilizing the inactive, iron-rich conformation via chaperone or scaffold properties, its deficiency leading to the basal accumulation of the iron starvation-induced conformation. However, it is difficult to reconcile this putative chaperone role of Pfh1 on Grx4 activity when the first protein has mitochondrial localization (Fig. 2F) and Grx4 displays cytoplasmic and nuclear localization (our own unpublished data). Our results unambiguously indicate that the absence of *S. pombe* frataxin causes a real iron starvation situation able to trigger the complex up- and down-regulation of the gene expression program. Indeed, activation of a complete iron starvation response, including up-regulation of the high-affinity iron transport system Fet3-Ftr1 and increased rate of iron uptake, has been described before in the yeast model of Friedreich ataxia (10). Furthermore, both increased iron uptake and a decrease in the major pathways of mitochondrial iron utilization have been described in a mice model of Friedreich ataxia (51). A possible role for frataxin which nicely fits with these results is its participation in the regulation of cellular iron homeostasis from the mitochondria. Maybe Pfh1 depletion triggers accumulation of the metal in this compartment, with the concomitant decrease of available cytosolic iron, and Grx4 activation. Further experiments to confirm this hypothesis are of course required.

Our study also strongly suggests that constitutive repression of many essential ISC-containing proteins in strain *Δpfh1* contributes to the severe phenotypes observed, since they can be partially suppressed by deletion of *php4* (Fig. 5BC). Studies on our new *S. pombe* model system on Friedreich ataxia will hopefully contribute to understanding the function of frataxin and to easily test different therapeutic interventions, which may prevent the onset of the disease.

REFERENCES

1. Harding, A. E. (1981) Friedreich's ataxia: a clinical and genetic study of 90 families with an analysis of early diagnostic criteria and intrafamilial clustering of clinical features. *Brain* **104**, 589-620
2. Campuzano, V., Montermini, L., Molto, M. D., Pianese, L., Cossee, M., Cavalcanti, F., Monros, E., Rodius, F., Duclos, F., Monticelli, A., Zara, F., Canizares, J., Koutnikova, H., Bidichandani, S. I., Gellera, C., Brice, A., Trouillas, P., De Michele, G., Filla, A., De Frutos, R., Palau, F., Patel, P. I., Di Donato, S., Mandel, J. L., Cocozza, S., Koenig, M., and Pandolfo, M. (1996) Friedreich's ataxia: autosomal recessive disease caused by an intronic GAA triplet repeat expansion. *Science* **271**, 1423-1427
3. Puccio, H., and Koenig, M. (2000) Recent advances in the molecular pathogenesis of Friedreich ataxia. *Hum Mol Genet* **9**, 887-892
4. Hausse, A. O., Aggoun, Y., Bonnet, D., Sidi, D., Munnich, A., Rotig, A., and Rustin, P. (2002) Idebenone and reduced cardiac hypertrophy in Friedreich's ataxia. *Heart* **87**, 346-349
5. Armstrong, J. S., Khdour, O., and Hecht, S. M. (2010) Does oxidative stress contribute to the pathology of Friedreich's ataxia? A radical question. *Faseb J* **24**, 2152-2163
6. Bradley, J. L., Blake, J. C., Chamberlain, S., Thomas, P. K., Cooper, J. M., and Schapira, A. H. (2000) Clinical, biochemical and molecular genetic correlations in Friedreich's ataxia. *Hum Mol Genet* **9**, 275-282
7. Rotig, A., de Lonlay, P., Chretien, D., Foury, F., Koenig, M., Sidi, D., Munnich, A., and Rustin, P. (1997) Aconitase and mitochondrial iron-sulphur protein deficiency in Friedreich ataxia. *Nat Genet* **17**, 215-217
8. Lamarche, J. B., Cote, M., and Lemieux, B. (1980) The cardiomyopathy of Friedreich's ataxia morphological observations in 3 cases. *Can J Neurol Sci* **7**, 389-396
9. Puccio, H., Simon, D., Cossee, M., Criqui-Filipe, P., Tiziano, F., Melki, J., Hindelang, C., Matyas, R., Rustin, P., and Koenig, M. (2001) Mouse models for Friedreich ataxia exhibit cardiomyopathy, sensory nerve defect and Fe-S enzyme deficiency followed by intramitochondrial iron deposits. *Nat Genet* **27**, 181-186
10. Babcock, M., de Silva, D., Oaks, R., Davis-Kaplan, S., Jiralerspong, S., Montermini, L., Pandolfo, M., and Kaplan, J. (1997) Regulation of mitochondrial iron accumulation by Yfh1p, a putative homolog of frataxin. *Science* **276**, 1709-1712
11. Kaplan, C. D., and Kaplan, J. (2009) Iron acquisition and transcriptional regulation. *Chem Rev* **109**, 4536-4552
12. Halliwell, B., and Gutteridge, J. M. (1984) Oxygen toxicity, oxygen radicals, transition metals and disease. *Biochem J* **219**, 1-14
13. Cornelis, P., Wei, Q., Andrews, S. C., and Vinckx, T. (2011) Iron homeostasis and management of oxidative stress response in bacteria. *Metallomics* **3**, 540-549
14. Pandolfo, M., and Pastore, A. (2009) The pathogenesis of Friedreich ataxia and the structure and function of frataxin. *J Neurol* **256 Suppl 1**, 9-17
15. Wilson, R. B., and Roof, D. M. (1997) Respiratory deficiency due to loss of mitochondrial DNA in yeast lacking the frataxin homologue. *Nat Genet* **16**, 352-357
16. Foury, F., and Cazzalini, O. (1997) Deletion of the yeast homologue of the human gene associated with Friedreich's ataxia elicits iron accumulation in mitochondria. *FEBS Lett* **411**, 373-377
17. Lesuisse, E., Santos, R., Matzanke, B. F., Knight, S. A., Camadro, J. M., and Dancis, A. (2003) Iron use for haeme synthesis is under control of the yeast frataxin homologue (Yfh1). *Hum Mol Genet* **12**, 879-889
18. Yoon, T., and Cowan, J. A. (2003) Iron-sulfur cluster biosynthesis. Characterization of frataxin as an iron donor for assembly of [2Fe-2S] clusters in ISU-type proteins. *J Am Chem Soc* **125**, 6078-6084

19. Gerber, J., Muhlenhoff, U., and Lill, R. (2003) An interaction between frataxin and Isu1/Nfs1 that is crucial for Fe/S cluster synthesis on Isu1. *EMBO Rep* **4**, 906-911
20. Muhlenhoff, U., Richhardt, N., Ristow, M., Kispal, G., and Lill, R. (2002) The yeast frataxin homolog Yfh1p plays a specific role in the maturation of cellular Fe/S proteins. *Hum Mol Genet* **11**, 2025-2036
21. Moreno-Cermeno, A., Obis, E., Belli, G., Cabiscol, E., Ros, J., and Tamarit, J. (2010) Frataxin depletion in yeast triggers up-regulation of iron transport systems before affecting iron-sulfur enzyme activities. *J Biol Chem* **285**, 41653-41664
22. Corpet, F. (1988) Multiple sequence alignment with hierarchical clustering. *Nucleic Acids Res* **16**, 10881-10890
23. Alfa, C., Fantes, P., Hyams, J., McLeod, M., and Warbrick, E. (1993) *Experiments with Fission Yeast: A Laboratory Course Manual*, Cold Spring Harbor Laboratory, Cold Spring Harbor, N.Y.
24. Leupold, U. (1970) Genetical methods for *Schizosaccharomyces pombe*. *Methods Cell Physiol.* **4**, 169-177
25. Zuin, A., Vivancos, A. P., Sanso, M., Takatsume, Y., Ayte, J., Inoue, Y., and Hidalgo, E. (2005) The glycolytic metabolite methylglyoxal activates Pap1 and Sty1 stress responses in Schizosaccharomyces pombe. *J Biol Chem* **280**, 36708-36713
26. Bahler, J., Wu, J. Q., Longtine, M. S., Shah, N. G., McKenzie, A., III, Steever, A. B., Wach, A., Philippsen, P., and Pringle, J. R. (1998) Heterologous modules for efficient and versatile PCR-based gene targeting in Schizosaccharomyces pombe. *Yeast* **14**, 943-951
27. Hentges, P., Van Driessche, B., Tafforeau, L., Vandenhaute, J., and Carr, A. M. (2005) Three novel antibiotic marker cassettes for gene disruption and marker switching in Schizosaccharomyces pombe. *Yeast* **22**, 1013-1019
28. Castillo, E. A., Vivancos, A. P., Jones, N., Ayte, J., and Hidalgo, E. (2003) Schizosaccharomyces pombe cells lacking the Ran-binding protein Hba1 show a multidrug resistance phenotype due to constitutive nuclear accumulation of Pap1. *J Biol Chem* **278**, 40565-40572
29. Kim, D. U., Hayles, J., Kim, D., Wood, V., Park, H. O., Won, M., Yoo, H. S., Duhig, T., Nam, M., Palmer, G., Han, S., Jeffery, L., Baek, S. T., Lee, H., Shim, Y. S., Lee, M., Kim, L., Heo, K. S., Noh, E. J., Lee, A. R., Jang, Y. J., Chung, K. S., Choi, S. J., Park, J. Y., Park, Y., Kim, H. M., Park, S. K., Park, H. J., Kang, E. J., Kim, H. B., Kang, H. S., Park, H. M., Kim, K., Song, K., Song, K. B., Nurse, P., and Hoe, K. L. (2010) Analysis of a genome-wide set of gene deletions in the fission yeast Schizosaccharomyces pombe. *Nat Biotechnol* **28**, 617-623
30. Calvo, I. A., Gabrielli, N., Iglesias-Baena, I., Garcia-Santamarina, S., Hoe, K. L., Kim, D. U., Sanso, M., Zuin, A., Perez, P., Ayte, J., and Hidalgo, E. (2009) Genome-wide screen of genes required for caffeine tolerance in fission yeast. *PLoS One* **4**, e6619
31. Garcia-Santamarina, S., Boronat, S., Espadas, G., Ayte, J., Molina, H., and Hidalgo, E. (2011) The oxidized thiol proteome in fission yeast--optimization of an ICAT-based method to identify H2O2-oxidized proteins. *J Proteomics* **74**, 2476-2486
32. Tamarit, J., Irazusta, V., Moreno-Cermeno, A., and Ros, J. (2006) Colorimetric assay for the quantitation of iron in yeast. *Anal Biochem* **351**, 149-151
33. Chaudhuri, A. R., de Waal, E. M., Pierce, A., Van Remmen, H., Ward, W. F., and Richardson, A. (2006) Detection of protein carbonyls in aging liver tissue: A fluorescence-based proteomic approach. *Mech Ageing Dev* **127**, 849-861
34. Hausladen, A., and Fridovich, I. (1996) Measuring nitric oxide and superoxide: rate constants for aconitase reactivity. *Methods Enzymol* **269**, 37-41
35. Zuin, A., Carmona, M., Morales-Ivorra, I., Gabrielli, N., Vivancos, A. P., Ayte, J., and Hidalgo, E. (2010) Lifespan extension by calorie restriction relies on the Sty1 MAP kinase stress pathway. *Embo J* **29**, 981-991
36. Vivancos, A. P., Castillo, E. A., Jones, N., Ayte, J., and Hidalgo, E. (2004) Activation of the redox sensor Pap1 by hydrogen peroxide requires modulation of the intracellular oxidant concentration. *Mol Microbiol* **52**, 1427-1435

37. Castillo, E. A., Ayte, J., Chiva, C., Moldon, A., Carrascal, M., Abian, J., Jones, N., and Hidalgo, E. (2002) Diethylmaleate activates the transcription factor Pap1 by covalent modification of critical cysteine residues. *Mol Microbiol* **45**, 243-254
38. Sanso, M., Gogol, M., Ayte, J., Seidel, C., and Hidalgo, E. (2008) Transcription factors Pcr1 and Atf1 have distinct roles in stress- and Sty1-dependent gene regulation. *Eukaryot Cell* **7**, 826-835
39. Hsu, J. L., Huang, S. Y., Chow, N. H., and Chen, S. H. (2003) Stable-isotope dimethyl labeling for quantitative proteomics. *Anal Chem* **75**, 6843-6852
40. Boersema, P. J., Raijmakers, R., Lemeer, S., Mohammed, S., and Heck, A. J. (2009) Multiplex peptide stable isotope dimethyl labeling for quantitative proteomics. *Nat Protoc* **4**, 484-494
41. Mercier, A., Watt, S., Bahler, J., and Labbe, S. (2008) Key function for the CCAAT-binding factor Php4 to regulate gene expression in response to iron deficiency in fission yeast. *Eukaryot Cell* **7**, 493-508
42. Chen, D., Wilkinson, C. R., Watt, S., Penkett, C. J., Toone, W. M., Jones, N., and Bahler, J. (2008) Multiple pathways differentially regulate global oxidative stress responses in fission yeast. *Mol Biol Cell* **19**, 308-317
43. Calvo, I. A., Garcia, P., Ayte, J., and Hidalgo, E. (2012) The transcription factors Pap1 and Prr1 collaborate to activate antioxidant, but not drug tolerance, genes in response to H2O2. *Nucleic Acids Res* **40**, 4816-4824
44. Mercier, A., Pelletier, B., and Labbe, S. (2006) A transcription factor cascade involving Fep1 and the CCAAT-binding factor Php4 regulates gene expression in response to iron deficiency in the fission yeast Schizosaccharomyces pombe. *Eukaryot Cell* **5**, 1866-1881
45. Jbel, M., Mercier, A., Pelletier, B., Beaudoin, J., and Labbe, S. (2009) Iron activates in vivo DNA binding of Schizosaccharomyces pombe transcription factor Fep1 through its amino-terminal region. *Eukaryot Cell* **8**, 649-664
46. Mercier, A., and Labbe, S. (2009) Both Php4 function and subcellular localization are regulated by iron via a multistep mechanism involving the glutaredoxin Grx4 and the exportin Crm1. *J Biol Chem* **284**, 20249-20262
47. Foury, F. (1999) Low iron concentration and aconitase deficiency in a yeast frataxin homologue deficient strain. *FEBS Lett* **456**, 281-284
48. Wang, T., and Craig, E. A. (2008) Binding of yeast frataxin to the scaffold for Fe-S cluster biogenesis, Isu. *J Biol Chem* **283**, 12674-12679
49. Bulteau, A. L., Dancis, A., Gareil, M., Montagne, J. J., Camadro, J. M., and Lesuisse, E. (2007) Oxidative stress and protease dysfunction in the yeast model of Friedreich ataxia. *Free Radic Biol Med* **42**, 1561-1570
50. Chen, O. S., and Kaplan, J. (2000) CCC1 suppresses mitochondrial damage in the yeast model of Friedreich's ataxia by limiting mitochondrial iron accumulation. *J Biol Chem* **275**, 7626-7632
51. Huang, M. L., Becker, E. M., Whitnall, M., Suryo Rahmanto, Y., Ponka, P., and Richardson, D. R. (2009) Elucidation of the mechanism of mitochondrial iron loading in Friedreich's ataxia by analysis of a mouse mutant. *Proc Natl Acad Sci U S A* **106**, 16381-16386
52. Pelletier, B., Beaudoin, J., Mukai, Y., and Labbe, S. (2002) Fep1, an iron sensor regulating iron transporter gene expression in Schizosaccharomyces pombe. *J Biol Chem* **277**, 22950-22958

Acknowledgments - We thank members of the laboratories of Joaquim Ros and Jordi Tamarit for helpful discussions. The authors thank Mercè Carmona for technical assistance. We are grateful to the joint CRG-UPF Proteomic Facility (Barcelona, Spain), where the mass spectrometry experiments were performed, and in particular to Henrik Molina and Guadalupe Espadas.

FOOTNOTES

*****This work was supported by the Spanish Ministry of Science and Innovation (BFU2009-06933, BFU2012-32045), PLAN E and FEDER, by the Spanish program Consolider-Ingenio 2010 Grant CSD 2007-0020, and by SGR2009-196 from Generalitat de Catalunya (Spain) to E.H. E. H. and J.A. are recipients of ICREA Academia Awards (Generalitat de Catalunya).

[S]This article contains supplemental Tables 1-5 and supplemental Fig. 1.

[1]To whom correspondence should be addressed: Universitat Pompeu Fabra, C/ Dr. Aiguader 88, 08003 Barcelona, Spain, Tel.: 34-93-316-0848; Fax.: 34-93-316-0901; E-mail: elena.hidalgo@upf.edu.

[1]The abbreviations used are: ISC, iron-sulfur cluster; ROS, reactive oxygen species; ORF, open reading frame; GFP, green fluorescent protein; Dx, deferroxamine; DIP, dipyridyl; H_2O_2, hydrogen peroxide; TCA, trichloroacetic acid.

FIG. LEGENDS

FIG. 1. Identification and characterization of *pfh1,* the frataxin homolog gene in *S. pombe*. *A*. Amino acid (aa) alignment of the frataxin homologs in *S. pombe* and *S. cerevisiae* with human isoform1 frataxin sequence. In red letters are represented the consensus sequence of aa that are conserved in the three organisms, and in blue letters are written the amino acid sequence that are present just in two of the organism. The phylogenetic tree relative to the frataxin gene for these organisms is represented in the right panel. *B*. Northern blot analysis of *pfh1* mRNA. Total RNA from strains 972 (WT) and NG60 (Δ*pfh1*) was obtained from cultures growing anaerobically. The RNA was analyzed by Northern blot using a *pfh1* probe. Total ribosomal RNA was used as a loading control. *C*. Cells lacking Pfh1 displays severely compromised aerobic growth. Strains 972 (WT) and NG60 (Δ*pfh1*) were grown anaerobically in YE5S to a final OD_{600} of 0.5, and serial dilutions from 10^5 to 10 cells were spotted in duplicate into YE5S plates and incubated at 30°C for 2-3 days in aerobic or anaerobic conditions. *D*. Viability of wild type (WT) and NG60 (Δ*pfh1*) cultures in response to aerobic growth. Strains 972 (WT) and NG60 (Δ*pfh1*) were grown overnight (ON) in YE5S in aerobic (**+ ON + O_2**) or anaerobic (**+ ON - O_2**) conditions, and then serial dilutions of logarithmic phase cells were spotted as described in *C;* plates were grown under anaerobic conditions (-O_2 plate). *E*. Pfh1 is sensitive to H_2O_2 stress. Survival of wild type (WT), AV18 (Δ*sty1*) and NG60 (Δ*pfh1*) strains in response to the indicated concentration of H_2O_2 in plates under anaerobic conditions.

FIG. 2. Phenotypic characterization of strain Δ*pfh1*. *A*. Total iron concentration of wild type (WT) and NG60 (Δ*pfh1*) strains were measured as indicated in Experimental Procedures. *B*. Reversible oxidized thiols are high in cells lacking Pfh1. Oxidized thiol labeling of wild type (WT) and NG60 (Δ*pfh1*) extracts was analyzed by fluorescent 1D gel electrophoresis (see Experimental Procedures) in anaerobic or aerobic conditions. Silver staining was used as control of protein loading. *C*. Protein carbonylation is high in extracts from Δ*pfh1* strain. Strains 972 (WT) and NG60 (Δ*pfh1*) were grown aerobically for 3 h to a final OD_{600} of 0.5, and protein carbonylation was detected as described in Experimental Procedures. Silver staining was used as a control of protein loading. *D*. The activity of the ISC-containing protein aconitase is impaired in a Δ*pfh1* strain. Aconitase activity of 972 (WT) and NG60 (Δ*pfh1*) strains was performed as indicated in Experimental Procedures. *E*. The respiratory rate of strain Δ*pfh1* is diminished. Oxygen consumption of 972 (WT) and NG60 (Δ*pfh1*) cells grown in YE5S under anaerobic conditions was measured as is indicated in Experimental Procedures. Data in A, D and E panels was obtained from three independent experiments and are expressed as mean ± SEM (standard error of the mean). Significant differences in A, D and E panels between wild-type and Δ*pfh1* cells were determined by Student's *t*-test, (**P*<0.05 and ***P*<0.01). *F*. Mitochondrial localization of Pfh1-GFP protein. Strain NG142 (expressing Pfh1-GFP) was grown under aerobic conditions. Cells were incubated with the mitochondrial dye Mitotracker Red prior to analysis. The cellular distribution of the fusion protein (green; Pfh1-GFP) and the dye (red; Mitotracker) was determined by fluorescence microscopy. The same cells under differential interference contrast (Nomarski) optics are shown in the bottom panel.

FIG. 3. Cells lacking *pfh1* over-express a subset of Pap1-dependent genes. *A*. Scheme of the activation of Pap1 pathway in *S. pombe* wild type cells. Pap1 activates two subsets of genes, the antioxidant and the drug resistance genes. In wild-type cells, oxidation of Pap1 upon H_2O_2 stress induces its nuclear accumulation and a heterodimer with Prr1 is formed, which is able to activate both sets of promoters, the antioxidant (*trr1, srx1, ctt1*) and the drug resistance (*obr1, caf5, c663.08c*) genes. *B*. Northern blot analysis of Pap1-dependent genes. Total RNA from strains 972 (WT) and NG60 (Δ*pfh1*) was obtained from cultures growing anaerobically or shifted to aerobic conditions for the times indicated, and treated or not H_2O_2. The RNA was analyzed by Northern blot using the probes indicated in the Fig. Total ribosoma RNA was used as a loading control. *C*. Northern blot analysis of *pap1* gene. Total RNA from strains 972

(WT) and NG60 (Δ*pfh1*) strains was obtained from cultures growing anaerobically or aerobically. The *pap1* ORF was used as a probe. *D*. The amount of Pap1 protein is higher in a Δ*pfh1* than in wild type cells. Total TCA protein extracts were analyzed by Western blot with anti-Pap1 antibodies; anti-Sty1 antibodies was use as a loading control. *E*. Hypothetical scheme of Pap1 activation in Δ*pfh1* cells. T here is an accumulation of reduced Pap1 that is able to enter in the nucleus and activate the drug resistance genes.

FIG. 4. Cells lacking Pfh1 show increased expression of proteins normally up-regulated in response to iron starvation. *A*. Scheme of iron starvation response in *S. pombe* cells. Grx4 is a glutaredoxin whose role is to sense the iron levels in the cells, and transmit the iron status to two repressor factors, Fep1 and Php4. Fep1 is the repressor of the iron up-take genes and Php4 is a protein that represses a set of genes that code for iron-containing proteins and iron storage. *B*. Northern blot analysis of Fep1-dependent genes. Total RNA from strains 972 (WT), NG60 (Δ*pfh1*), NG1 (Δ*fep1*) and NG147 (Δ*pfh1* Δ*fep1*) was obtained from cultures growing in YE5S aerobically for 90 min treated or not with 250 μM of the iron chelator DIP. *C*. The aerobic growth defects of strain Δ*pfh1* is not due to the increment in the iron up-take system. Strains 972 (WT), NG60 (Δ*pfh1*), NG1 (Δ*fep1*) and NG147 (Δ*pfh1* Δ*fep1*) were grown in YE plates under aerobic or anaerobic conditions, as described in Fig. 1C. *D*. Growth curves of 972 (WT), NG60 (Δ*pfh1*) and NG1 (Δ*fep1*) strains were done in YE5S liquid medium and OD_{600} was recorded at the indicated times for each culture during 35h.

FIG. 5. Cells lacking Pfh1 down-regulate genes normally down-regulated under iron starvation. *A*. Genes coding for iron containing proteins (such as *isa1*) or involved in iron storage (such as pcl1) are down regulated in a Δ*pfh1* strain. Total RNA from strains 972 (WT), NG60 (Δ*pfh1*), NG40 (Δ*php4*) and NG148 (Δ*pfh1* Δ*php4*) was obtained from cultures growing in YE5S aerobically for 90 min treated or not with 250 μM of DIP. Northern blot analysis of Php4-dependent genes was performed. *B*. Deletion of the *php4* gene partially suppresses the aerobic defects of strain Δ*pfh1*. Survival spots were performed for 972 (WT), NG60 (Δ*pfh1*), NG40 (Δ*php4*) and NG148 (Δ*pfh1* Δ*php4*) strains in different agents under aerobic and anaerobic conditions. Those strains were grown in YE5S under anaerobic conditions to a final OD_{600} of 0.5 and then spotted in solid plates of low iron conditions (Dx) or high iron concentrations (Fe), at the indicated concentrations. *C*. Growth curves of 972 (WT), NG60 (Δ*pfh1*), NG40 (Δ*php4*) and NG148 (Δ*pfh1* Δ*php4*) strains were done in YE5S liquid medium and OD_{600} was recorded at the indicated time for each culture during 35 h.

FIG. 6. The transcriptome of Δ*pfh1* mimics that of Δ*grx4* Δ*fep1* cells. *A*. Northern blot analysis of Fep1- and Php4-dependent genes in different strain backgrounds. Total RNA from strains 972 (WT), NG60 (Δ*pfh1*), NG40 (Δ*php4*), NG1 (Δ*fep1*) and NG127 (Δ*grx4* Δ*fep1*) was obtained from cultures growing in YE5S aerobically for 90 min treated or not with 250 μM DIP. *B*. The double mutant Δ*grx4* Δfep1 is sensitive to growth under aerobic conditions. Survival spots were performed for 972 (WT), NG60 (Δ*pfh1*) and NG127 (Δ*grx4* Δ*fep1*) strains under aerobic and anaerobic conditions. Those strains were grown in YE5S under anaerobic conditions until to a final OD_{600} of 0.5 and then spotted in solid plates.

Table 1. Comparative quantification of Δ*pfh1 versus* wild-type proteome

	Proteins with altered expression in Δ*pfh1* vs WT	
	Number of proteins down-represented[a]	Number of proteins up-represented[b]
Proteins induced upon Fe starvation[c]	-	20[g]
Proteins repressed upon Fe starvation[d]	32	-
Proteins induced by nuclear Pap1[e]	-	9
Unknown[f]	39[e]	35[f]
Total	71	58

[a] Number of proteins down-regulated more than 2-fold in Δ*pfh1* versus wild-type cells after 3 hours under aerobic conditions.
[b] Number of proteins up-regulated more than 1.5-fold in Δ*pfh1* versus wild-type cells after 3 hours under aerobic conditions.
[c] The genes coding for these proteins are up-regulated upon iron starvation (41), probably in a Fep1-dependent manner (52).
[d] The genes coding for these proteins are down-regulated upon iron starvation, 23 of them in a Php4 dependent manner (41).
[e] The genes coding for these proteins are up-regulated in response to non-toxic doses of H_2O_2 in a Pap1 dependent manner (42).
[f] Number of proteins which regulation of expression is unknown.
[g] Six of these proteins are included in the set of proteins induced by Pap1.

Figure 1

Proteome of frataxin homolog in fission yeast

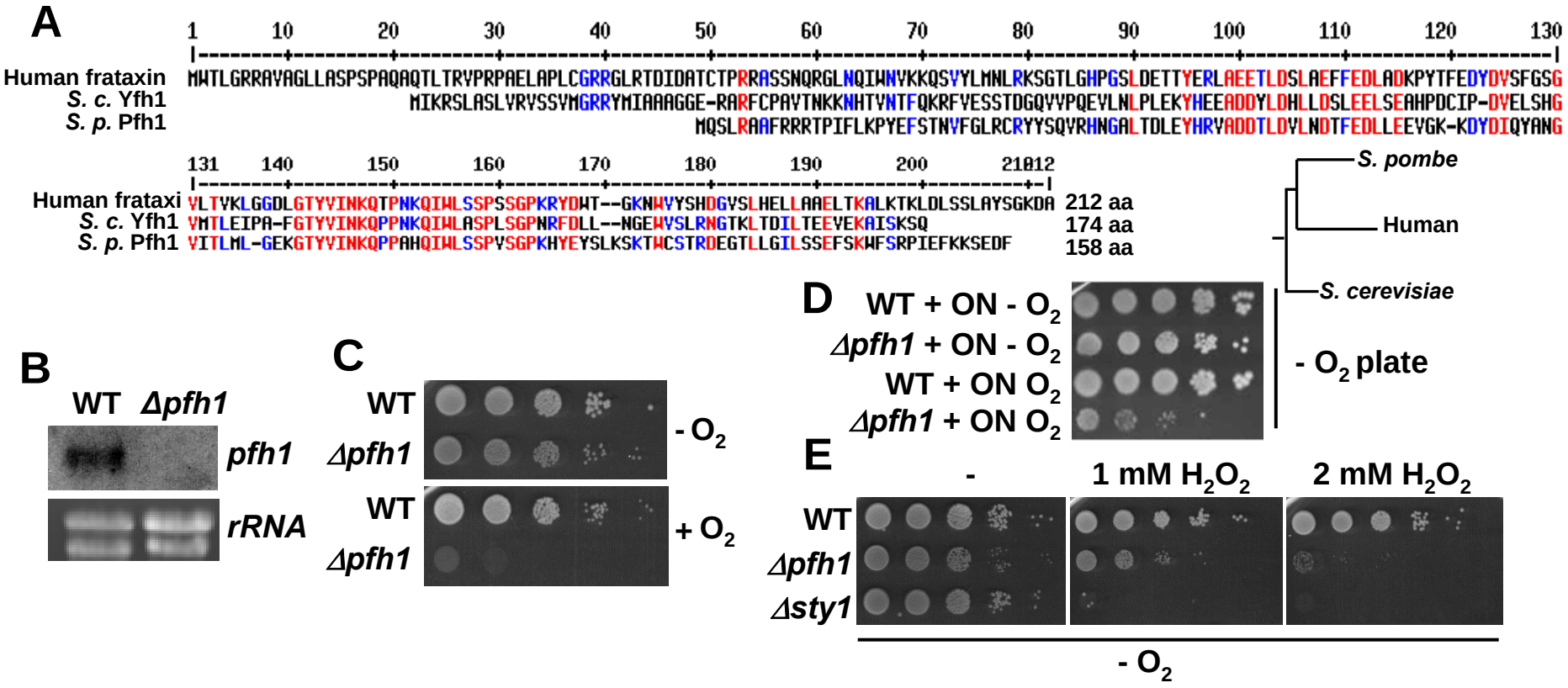

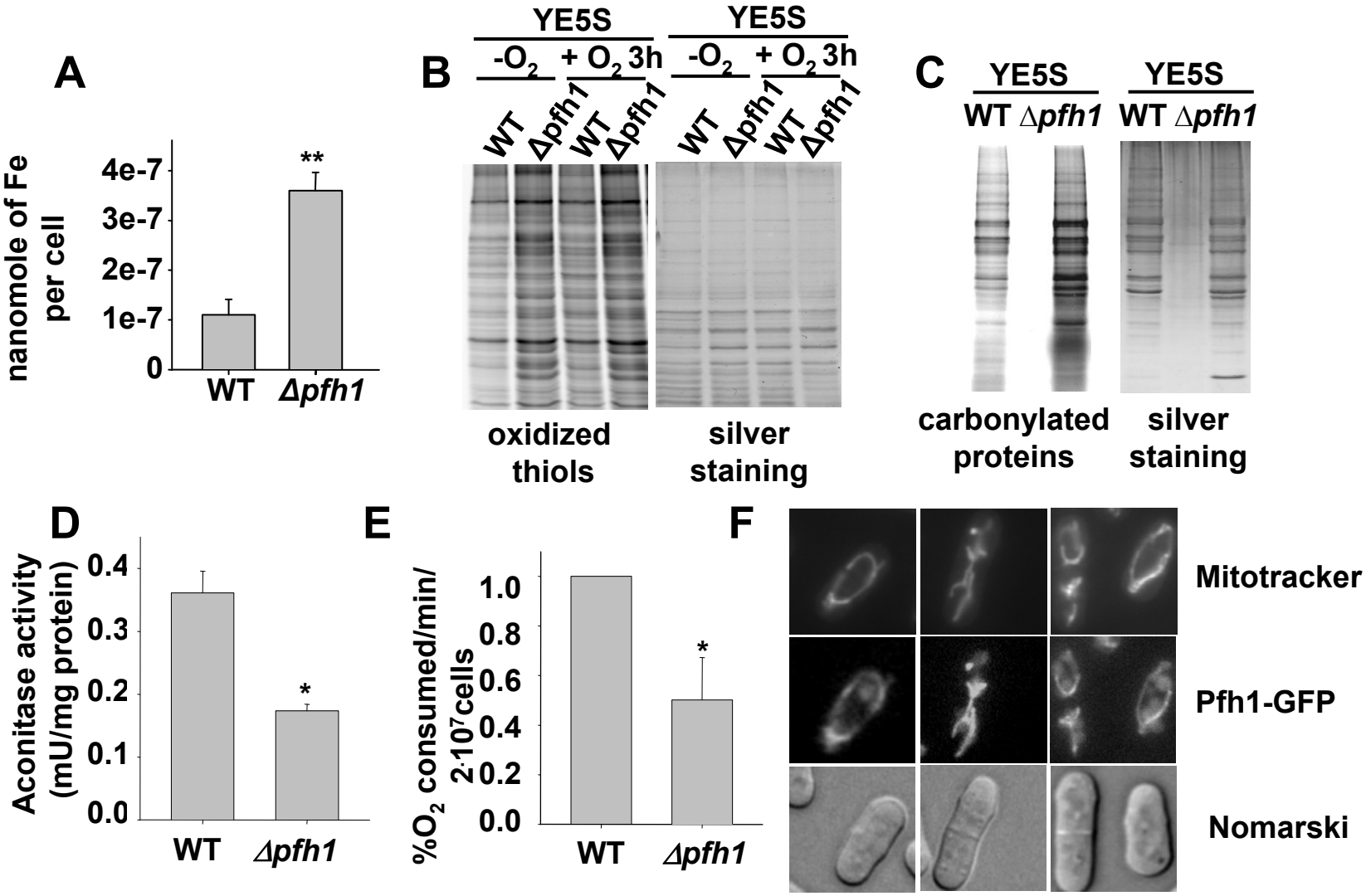
A
nanomole of Fe per cell
4e-7
3e-7
2e-7
1e-7
0
**
WT
Δpfh1
B
YE5S
-O2
+ O2 3h
YE5S
-O2
+ O2 3h
WT
Δpfh1
WT
Δpfh1
WT
Δpfh1
WT
Δpfh1
oxidized thiols
silver staining
C
YE5S
WT Δpfh1
YE5S
WT Δpfh1
carbonylated proteins
silver staining
D
Aconitase activity (mU/mg protein)
0.4
0.3
0.2
0.1
0.0
*
WT
Δpfh1
E
%O2 consumed/min/ 2·10^7cells
1.0
0.8
0.6
0.4
0.2
0.0
*
WT
Δpfh1
F
Mitotracker
Pfh1-GFP
Nomarski

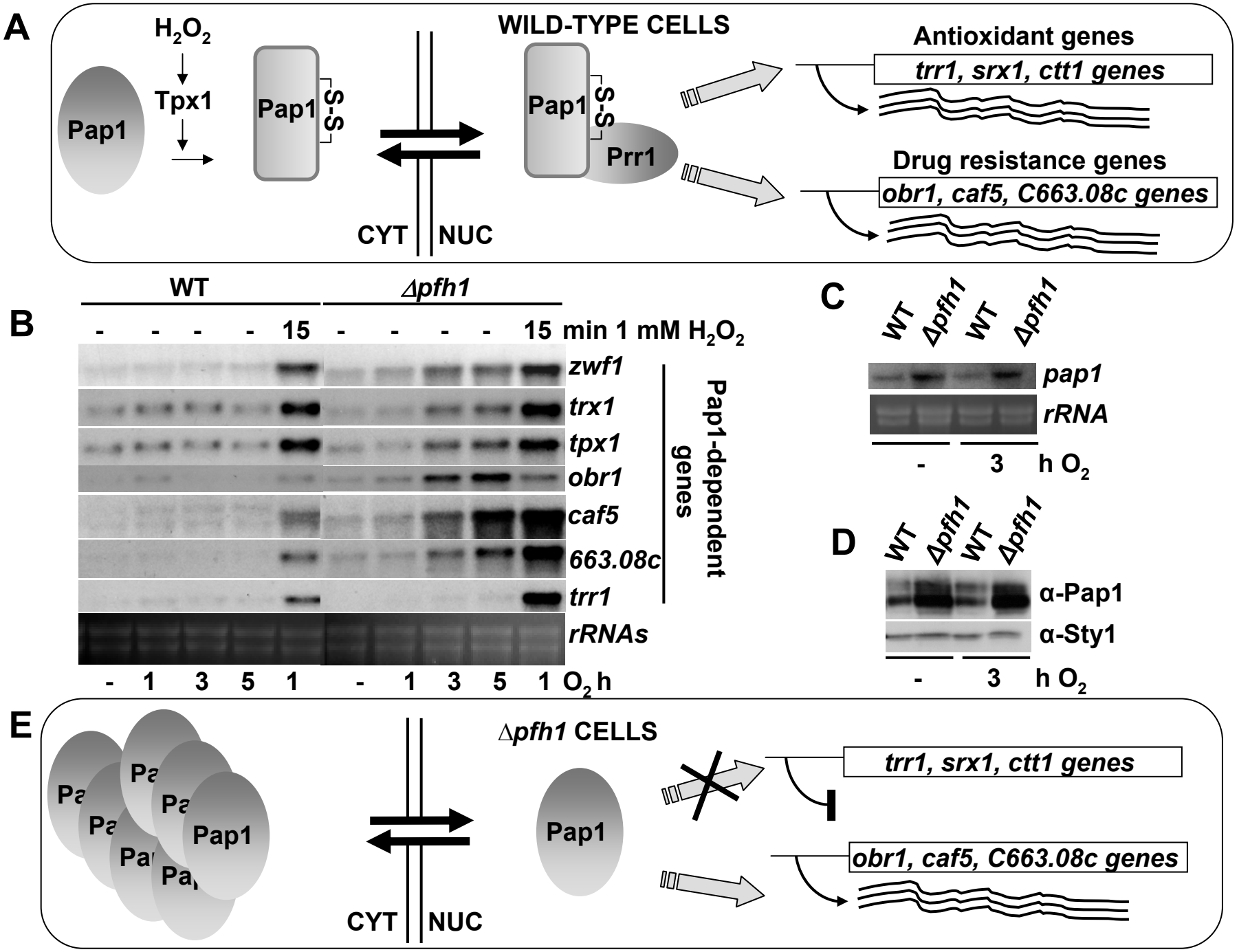
A
H_2O_2
Tpx1
Pap1
Pap1
S-S
CYT
NUC
WILD-TYPE CELLS
Pap1
S-S
Prr1
Antioxidant genes
trr1, srx1, ctt1 genes
Drug resistance genes
obr1, caf5, C663.08c genes
B
WT
Δpfh1
- - - - 15 - - - - 15 min 1 mM H_2O_2
zwf1
trx1
tpx1
obr1
caf5
663.08c
trr1
rRNAs
Pap1-dependent genes
- 1 3 5 1 - 1 3 5 1 O_2 h
C
WT
Δpfh1
WT
Δpfh1
pap1
rRNA
- 3 h O_2
D
WT
Δpfh1
WT
Δpfh1
α-Pap1
α-Sty1
- 3 h O_2
E
Pap1
CYT
NUC
Δpfh1 CELLS
Pap1
trr1, srx1, ctt1 genes
obr1, caf5, C663.08c genes

Figure 4

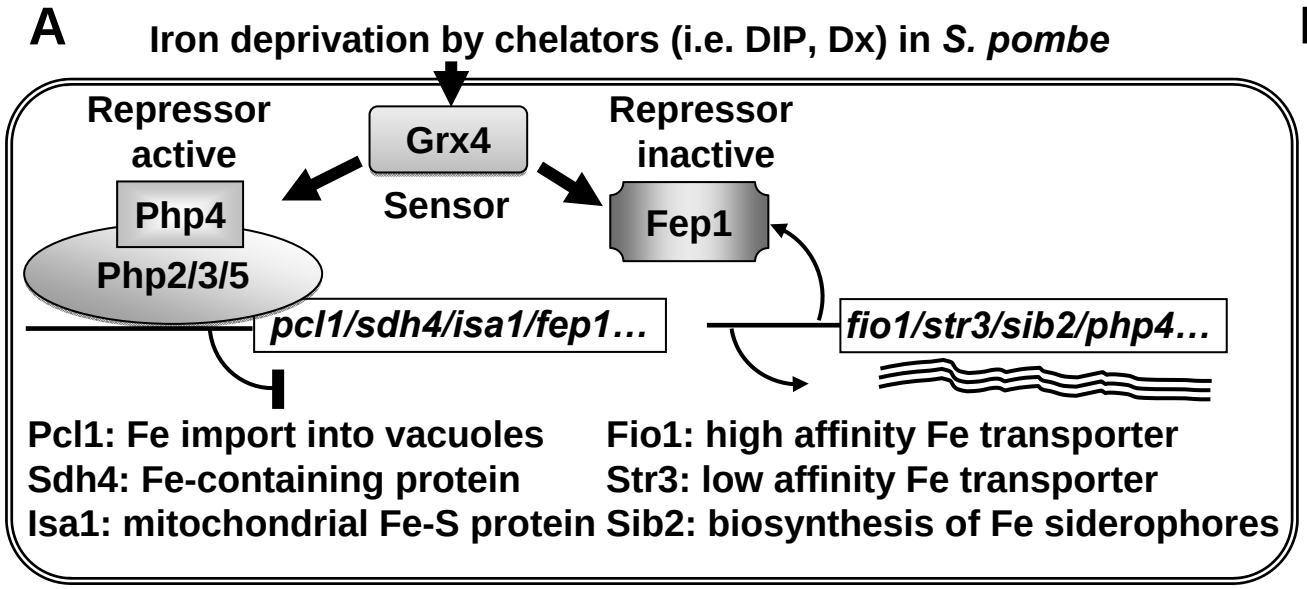
A
Iron deprivation by chelators (i.e. DIP, Dx) in S. pombe
Repressor active
Grx4
Sensor
Repressor inactive
Php4
Php2/3/5
Fep1
pcl1/sdh4/isa1/fep1…
fio1/str3/sib2/php4…
Pcl1: Fe import into vacuoles
Sdh4: Fe-containing protein
Isa1: mitochondrial Fe-S protein
Fio1: high affinity Fe transporter
Str3: low affinity Fe transporter
Sib2: biosynthesis of Fe siderophores

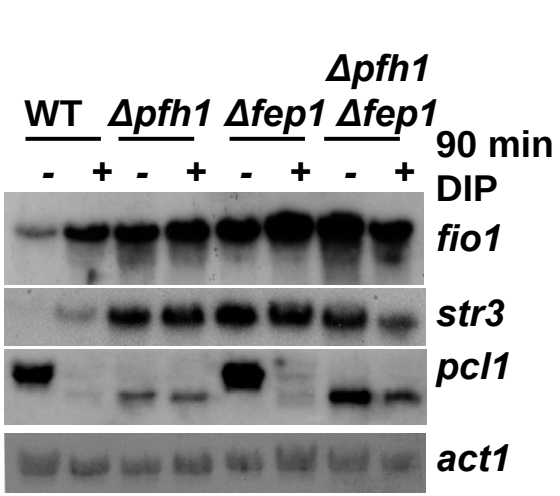
B
WT
Δpfh1
Δfep1
Δpfh1 Δfep1
90 min
- + - + - + - +
DIP
fio1
str3
pcl1
act1

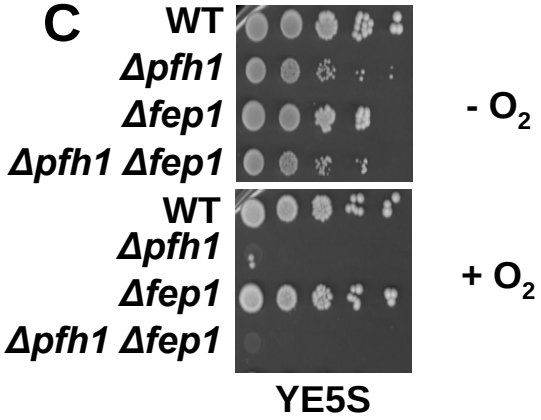
C
WT
Δpfh1
Δfep1
Δpfh1 Δfep1
- O2
WT
Δpfh1
Δfep1
Δpfh1 Δfep1
+ O2
YE5S

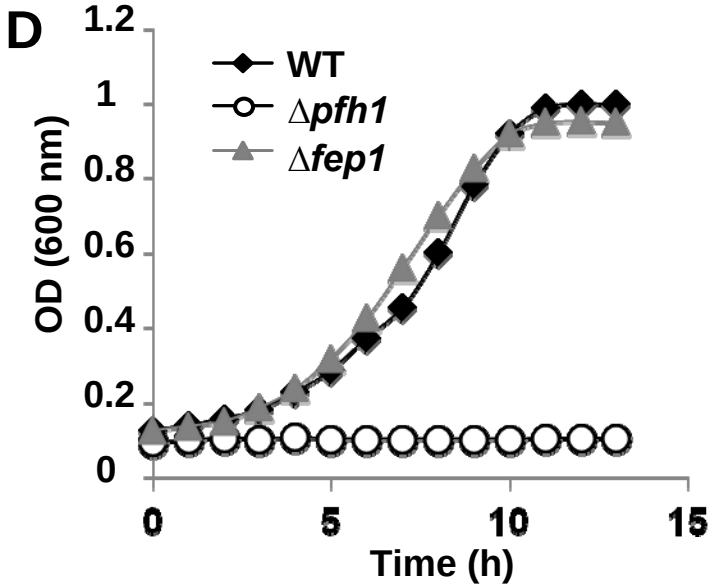
D
1.2
1
0.8
0.6
0.4
0.2
0
OD (600 nm)
WT
Δpfh1
Δfep1
0
5
10
15
Time (h)

Figure 5

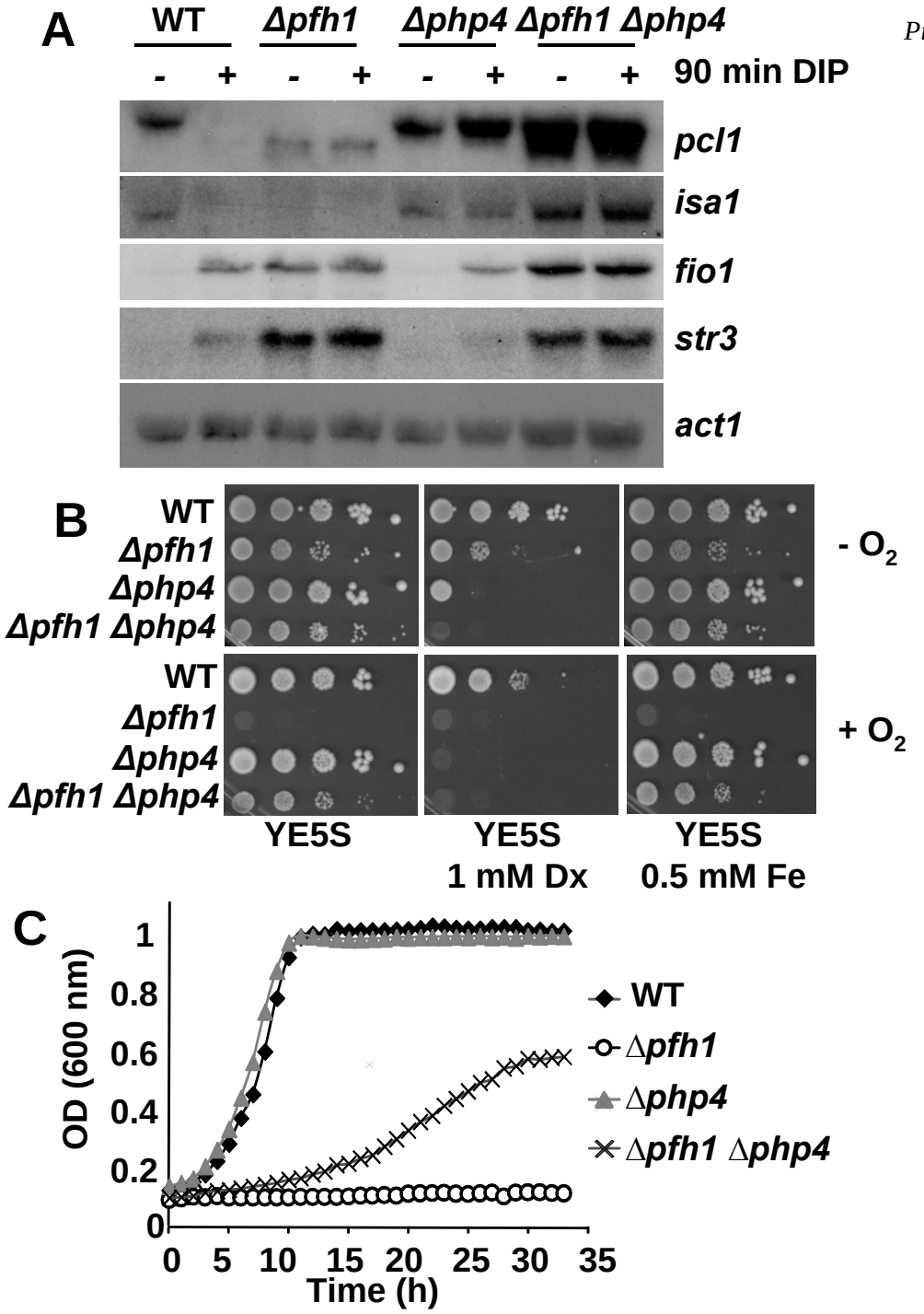
A
WT
Δpfh1
Δphp4
Δpfh1 Δphp4
- + - + - + - +
90 min DIP
pcl1
isa1
fio1
str3
act1
B
WT
Δpfh1
Δphp4
Δpfh1 Δphp4
- O2
+ O2
YE5S
YE5S
1 mM Dx
YE5S
0.5 mM Fe
C
OD (600 nm)
0
0.2
0.4
0.6
0.8
1
0 5 10 15 20 25 30 35
Time (h)
WT
Δpfh1
Δphp4
Δpfh1 Δphp4

Figure 6

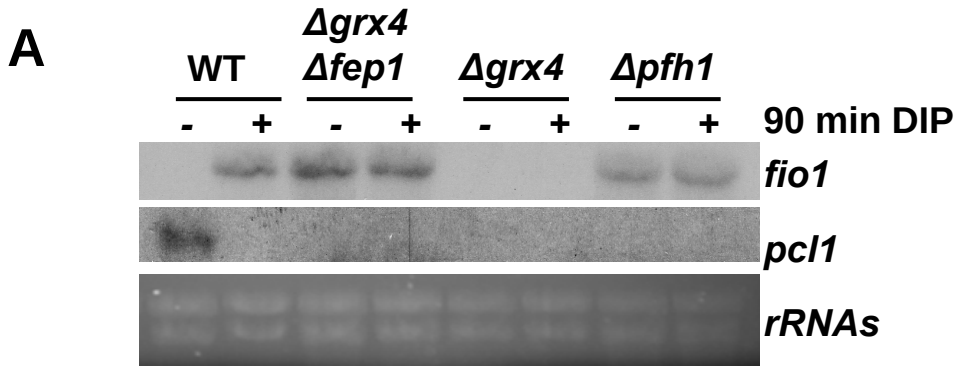
A
WT
Δgrx4 Δfep1
Δgrx4
Δpfh1
- + - + - + - +
90 min DIP
fio1
pcl1
rRNAs

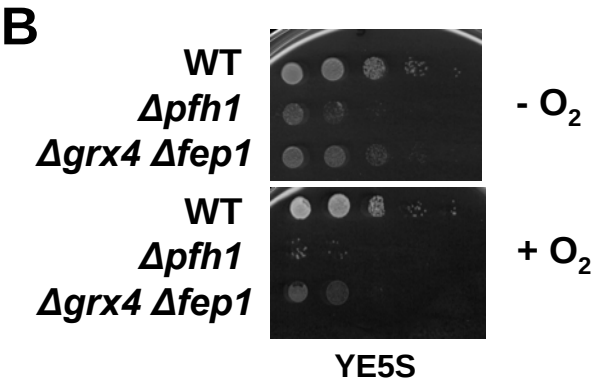
B
WT
Δpfh1
Δgrx4 Δfep1
- O2
WT
Δpfh1
Δgrx4 Δfep1
+ O2
YE5S